Soil Biology and Biochemistry 182 (2023) 109042

Contents lists available at ScienceDirect

Soil Biology and Biochemistry

journal homepage: www.elsevier.com/locate/soilbio

Decadal application of mineral fertilizers alters the molecular composition and origins of organic matter in particulate and mineral-associated fractions

Zhichao Zou [a], Lixiao Ma [a], Xiao Wang [a], Ruirui Chen [b], Davey L. Jones [c,d], Roland Bol [c,e], Di Wu [a,*], Zhangliu Du [a,**]

[a] Beijing Key Laboratory of Biodiversity and Organic Farming, College of Resources and Environmental Sciences, China Agricultural University, Beijing, 100083, China
[b] State Key Laboratory of Soil and Sustainable Agriculture, Institute of Soil Science, Chinese Academy of Sciences, Nanjing, 10008, China
[c] Environment Centre Wales, Bangor University, Gwynedd, LL57 2UW, UK
[d] SoilsWest, Centre for Sustainable Farming Systems, Food Futures Institute, Murdoch University, Murdoch, WA, 6105, Australia
[e] Institute of Bio- and Geosciences, Agrosphere (IBG-3), Forschungszentrum Jülich GmbH, 52425, Jülich, Germany

ARTICLE INFO

Keywords:
Mineral fertilizers
Soil organic matter
Biomarkers
Mineral-associated organic matter
Particulate organic matter

ABSTRACT

The extent to which long-term application of mineral fertilizers regulates the quantity, quality, and stability of soil organic matter (SOM) in soil matrices remains unclear. By combining four biomarkers, i.e., free and bound lipids, lignin phenols and amino sugars, we characterized the molecular composition, decomposition and origins of SOM in response to 10-year fertilization (400 kg N ha^{-1} yr^{-1}, 120 kg P ha^{-1} yr^{-1} and 50 kg K ha^{-1} yr^{-1}) in a cropland in North China. We focused on two contrasting fractions: particulate organic matter (POM), and mineral-associated organic matter (MAOM). Fertilization increased soil organic carbon (SOC) by 23% in MAOM, and altered its composition and origins, despite having a limited effect on bulk SOC levels. Fertilization increased plant-derived terpenoids by 46% in POM and long-chain lipids ($\geq C_{20}$) by 116% in MAOM but decreased short-chain lipids ($<C_{20}$) by 54% in the former fraction. Fertilization reduced suberin-derived lipids by 56% in POM and 30% in MAOM but increased lignin-derived phenols by 74% in POM and 31% in MAOM, implying that crop residues were preferentially stored via the POM form. Fertilization decreased the contribution of microbial residues to SOC in both the fractions. Overall, mineral fertilizers tended to reduce certain labile components within POM (e.g., short-chain lipids), leading to the accrual of recalcitrant molecules (e.g., long-chain lipids, cutin-derived lipids, and lignin-derived phenols) in the MAOM fraction. Collectively, our study suggests that mineral fertilizers can increase SOM stability and persistence by modifying their molecular composition and preservation in the mineral-organic associations in a temperate agroecosystem.

1. Introduction

Soil organic matter (SOM) is critical to a functioning agroecosystem because of its key role in maintaining soil fertility, promoting water retention, and soil organic carbon (SOC) sequestration (Hoffland et al., 2020; Kopittke et al., 2022). In typical croplands, large inputs of mineral fertilizers increase crop productivity (He et al., 2020; Cassman and Dobermann, 2022), leading to greater amounts of carbon entering the soil via residues, roots and their exudations, consequently regulating SOM turnover (Averill and Waring, 2018; Man et al., 2021). However, our fundamental understanding of the direction and magnitude of SOC stabilization and sequestration in response to nutrient fertilizers remains unclear. Previous studies have reported higher, neutral, and even lower SOC levels due to fertilizer management in agro-ecosystems (Khan et al., 2007; Ladha et al., 2011; Dou et al., 2016; Ni et al., 2022). In intensive agriculture, mineral fertilizers have been the key strategy to increase and/or maintain crop yields (Amelung et al., 2020). The observed nutrient-induced changes in SOC accrual have been related to i) the higher plant carbon input via increased litter and rhizodeposition (He et al., 2018; Singh and Benbi, 2018), ii) suppressed microbial metabolism and/or microbial biomass (Boot et al., 2016) and alteration in microbial community structure (Zhang et al., 2018; Ge et al., 2021;

* Corresponding author. College of Resources and Environmental Sciences, China Agricultural University, Beijing, 100193, China.
** Corresponding author. College of Resources and Environmental Sciences, China Agricultural University, Beijing, 100193, China.
E-mail addresses: d.wu@cau.edu.cn (D. Wu), dzl@cau.edu.cn (Z. Du).

https://doi.org/10.1016/j.soilbio.2023.109042
Received 14 February 2023; Received in revised form 17 April 2023; Accepted 19 April 2023
Available online 9 May 2023

Brown et al., 2022). The SOC accrual resulting from fertilizers may also be offset by the soil carbon loss from various soil fractions or the biodegradation of soil carbon, resulting in a zero or even negative accumulation of SOC (Dou et al., 2016; Man et al., 2021). Furthermore, mineral fertilizer inputs may modify SOM formation and stabilization via plant inputs, allocation pathways, and decomposition (Chenu et al., 2019; Song et al., 2019), thus altering its molecular composition and origins. Alongside the contrasting results on how fertilization influences SOC stocks, little information is available about how the application of mineral fertilizers affects the quality of SOM (e.g., molecules, lability, and sources).

Investigating the molecular composition of SOM could help uncover the origin and degradation pathway, thus contributing to assessing its lability and stability (Angst et al., 2021). An emerging view is that SOM represents a continuum of progressively decomposing organic compounds with various stages of biogeochemical degradation (Lehmann and Kleber, 2015). This complex mixture is composed of a range of biomolecules, such as polysaccharides, lipids, lignin, cutin, suberin, and amino sugars (Kögel-Knabner, 2002). Biomarker approaches have been shown to be a powerful tool for profiling SOM (Amelung et al., 2008; Gao et al., 2021; Ma et al., 2022a). For example, amino sugars and lignin phenols biomarkers have been used as distinct indicators of microbial- and plant-derived biomolecules (Thevenot et al., 2010; Joergensen, 2018; Liang et al., 2019). Moreover, long-chain free lipids ($\geq C_{20}$) and steroids are believed to be mainly plant-derived, whereas short-chain lipids ($<C_{20}$) and trehalose mainly originate from microbes (Bergen et al., 1998; Otto et al., 2005). Bound lipids, such as cutin and suberin, are plant-characterized biomacromolecules used to trace inputs from leaves and roots, respectively (Nierop et al., 2003; Otto and Simpson, 2006b; Hamer et al., 2012). However, most studies have focused on the effect of nutrition input (mostly nitrogen, N) in the natural systems and found N input could alter these SOM components and origins (Feng et al., 2010; Creme et al., 2017, 2018; Vandenenden et al., 2018). For instance, long-term N fertilization increased plant-derived lipids (e.g., steroids, cutin, and suberin) and lignin phenols in a temperate forest (Wang et al., 2019; Vandenenden et al., 2021) and grasslands (Creme et al., 2018). However, uncertainties remain as certain components, such as microbial residues, show inconsistent responses to fertilization (Liang and Balser, 2012; Zhang et al., 2016; Fan et al., 2020). Presumably, these varied results may be attributed to differences in fertilizer types, addition rates, duration, soil types, soil properties, ecosystems and climate regions (Treseder, 2008; Zhang et al., 2016; Ni et al., 2020; Ma et al., 2021, 2022b; Hu et al., 2022). However, few studies have investigated the molecular composition, origins, and stabilization of SOM in response to mineral fertilization in cropland soils, which is vital given their greater fertilizers inputs, higher rates of disturbances, lower SOC levels, and growing obligations to store more carbon in these soils to mitigate climate change.

Based on a simple framework, SOM can generally be fractionated into particulate organic matter (POM) and mineral-associated organic matter (MAOM) (Cotrufo et al., 2019; Samson et al., 2020). These two operational fractions are fundamentally distinct in term of their formation, persistence, and functioning (Lavallee et al., 2020; Witzgall et al., 2021). POM is inextricably linked to soil structure development and SOM stabilization (Six and Paustian, 2014), which mainly consists of relatively undecomposed plant fragments (Cotrufo et al., 2015). In contrast, partly decomposed POM can progressively transform into microbial by-products and adsorb onto the soil mineral surfaces to form MAOM, which represents the core of stable SOC (Liang et al., 2017; Hemingway et al., 2019; Sokol et al., 2019). MAOM mostly constitutes microbial-derived compounds (Ludwig et al., 2015) or equal plant- and microbial-derived biomolecules (Angst et al., 2021). These differences in function highlight the need to quantify and characterize POM and MAOM separately (Lavallee et al., 2020). Increasing evidences have shown that the soil and crop management practices could alter the amount and composition of SOM in the functional fractions (Kaiser and Ellerbrock, 2005; Chassé et al., 2021; Kauer et al., 2021; Zhang et al., 2022).

To the best of our knowledge, no study to date has specifically reported the response of SOM molecular composition and origins to long-term application of mineral fertilizer in POM and MAOM fractions in cropland soils. In the present study, we combined several key molecular-level biomarker techniques (e.g., free lipids, bound lipids, lignin-derived phenols, and amino sugars) to investigate the effect of decadal mineral fertilizers addition on the fate, degradation, and origins (e.g., plant- and microbial-derived) of functional POM and MAOM fractions from a temperate agroecosystem in North China. We hypothesized that: 1) mineral fertilizer application would increase the amount of SOM and lignin-derived phenols, while decreasing microbial residues, because of stimulated microbial necromass decay; and 2) nutrient-induced changes in SOM composition and origins would differ between POM and MAOM fractions, where POM would enrich plant-derived SOM, whereas MAOM would accumulate microbial residues.

2. Materials and methods

2.1. Site description, experimental design and soil sampling

A long-term field experiment was conducted at the Huantai Agroecosystem Experiment Station of China Agricultural University (117°58′E, 36°57′N), North China. The field site has a typical temperate continental monsoon climate with cold winters and hot summers. The mean annual temperature is approximately 12 °C and the mean annual precipitation is 540 mm, with most precipitation occurring from June to August. The dominant double-crop systems are winter wheat (early October to early June) and summer maize (middle June to late September). The tested soil was classified as a Fluvic Cambisols (USDA soil classification system), and it was a sandy loam texture (73% sand, 13% silt and 14% clay for the 0–20 cm depth).

The field experiment, established in July 2009, was laid out as a randomized block design with four treatments (three replicates, each 9m × 9m), two of which were chosen for the present study. The two treatments included an unfertilized control and mineral fertilizers application. In the fertilized plot, urea was applied at a total rate of 400 kg N ha^{-1} y^{-1}. Half of the urea was applied as a base fertilizer and the other half was topdressing. Specifically, urea was applied at a rate of 100 kg N ha^{-1} during the wheat sowing (October) and shooting (April) stages. The same rate was applied during the corn sowing (June) and growing season (August). In each fertilization plot, superphosphate was applied at 120 kg P ha^{-1} y^{-1} and potassium sulfate was applied at 50 kg K ha^{-1} y^{-1} when wheat was sown in October. After sowing, all plots were irrigated with 100 mm water.

Using a hand auger (with a diameter of 5 cm), soil cores (0–10 cm depth) were randomly collected at three locations from each plot in September 2019 and bulked to obtain a composite sample. This process was repeated for every plot. Subsequently, all soil samples were sieved (<2 mm) and visible stones and organic materials (e.g., fine roots) were removed before dividing each sample into two portions. One portion was air-dried for the determination of soil physicochemical properties, and another portion was freeze-dried for physical fractionation and further biomarker analysis. After removing inorganic carbon with diluted HCl (0.5 mol L^{-1}), the SOC and total nitrogen (TN) concentrations were determined using an elemental analyzer (vario MACRO cube, Germany).

Soil fractionation involves dispersing soil samples using low-energy sonication and separating the samples by wet sieving to obtain the POM and MAOM fractions (Cambardella and Elliott, 1992). Briefly, freeze-dried soil (50 g) was placed in a 500 mL beaker, and 250 mL of deionized water was added (soil/water ratio:5:1). The samples were dispersed in 270 J mL^{-1} for 15 min using an ultrasonic generator (SCIENTZ JY92-IIN, Ningbo, China). The suspension was passed through a 53-μm sieve to obtain these two fractions.

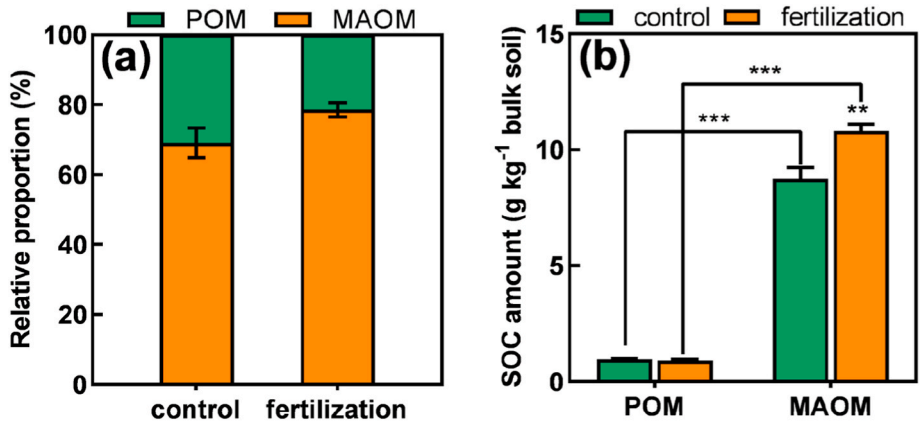

Fig. 1. Response of fraction mass proportion (a) and soil organic carbon (SOC) amount (b) changes in particulate organic matter (POM) and mineral-associated organic matter (MAOM) fractions as influenced by mineral fertilizers application. Values represent means ± SE (n = 3) for the control and fertilization treatments. *p < 0.05, **p < 0.01, and ***p < 0.001.

2.2. Targeted compounds identification and quantification

SOM biomarkers were extracted using a series of sequential chemical extractions (Otto et al., 2005). Freeze-dried soil samples were sonicated with organic solvents to extract free lipids, including *n*-alkanes, *n*-alkanols, *n*-alkanoic acids, and steroids. After solvent extraction, the soil residues were subjected to base hydrolysis to obtain bound lipids, which contained suberin-derived compounds (e.g., *ω*-hydroxy and dioic acids) and cutin-derived compounds (e.g., $C_{14\text{-}18}$ hydroxy- and epoxy acids). The remaining subsamples were air-dried and oxidized with CuO to release lignin-derived monomers, namely, vanillyl, syringyl, and cinnamyl compounds. Amino sugars were separated by HCl hydrolysis (Zhang and Amelung, 1996), including glucosamine (GluN), galactosamine (GalN), muramic acid (MurN), and mannosamine (ManN). After a successive series of extraction and chemical degradation procedures, the extracts were converted to trimethylsilyl and aldononitrile derivatives, respectively. The derivatized total extracts were analyzed using a gas chromatograph (GC; Agilent 7890B; Agilent Technologies, Santa Clara, CA, USA) equipped with a mass spectrometer (MS; Agilent 5977B, Agilent Technologies). The concentrations of individual extractable compounds were calculated by comparing their peak areas with those of the standards in the total ion current and then normalized to the mass of extracted soil. The detailed extraction procedures and quantification methods were provided in the Supplementary Material.

2.3. Biomarker parameters and calculations

Several molecular indicators have been used to assess the source and degradation stages of SOM at the molecular level. For example, free lipids (primarily *n*-alkanes, *n*-alkanols, and *n*-alkanoic acids) can be categorized into two clusters by their carbon atom numbers: short-chain ($<C_{20}$) and long-chain ($\geq C_{20}$) lipids. Plant-derived lipids include long-chain lipids and steroids (i.e., campesterol, stigmasterol and sitosterol), whereas microbial-derived SOM include short-chain lipids and trehalose (Otto et al., 2005; Amelung et al., 2008). Molecular proxies were used to reflect the degradation status of aliphatic lipids by assessing their carbon chain characteristics, such as the average chain length of *n*-alkanes (ACL_{Alk}), *n*-alkanoic acids (ACL_{Fa}), odd-over-even predominance values of *n*-alkanes (OEP_{Alk}) and even-over-odd predominance of *n*-alkanoic acids (EOP_{Fa}) (i.e., higher ACL values correspond to higher degradation) (Otto et al., 2005; Wiesenberg et al., 2010).

The decomposition of cutin-derived lipids was assessed by the ratio of C_{16} or C_{18} *ω*-hydroxy-alkanoic acids to all hydrolysable C_{16} or C_{18} aliphatic lipids (ω-$C_{16}/\Sigma C_{16}$ and ω-$C_{18}/\Sigma C_{18}$). Both parameters have been reported to increase with progressing cutin degradation (Otto and Simpson, 2006b; Feng and Simpson, 2007). Moreover, the ratio of mid-chain-substituted hydroxy and epoxy acids to total cutin-and suberin-derived compounds (Σmid/ΣSˆC) was calculated to reflect the degradation stage of suberin- and cutin-derived compounds. A decrease in this ratio implied progressive degradation of bound lipids (Otto and Simpson, 2006b). Detailed calculation information is provided in the Supplementary Material.

Lignin degradation was reflected by the acid/aldehyde (Ad/Al) ratios of the V and S units, which have been reported to increase with the progressive oxidation of lignin (Otto and Simpson, 2006a). According to the release efficiency in three types of lignin monomers, the plant-derived carbon in SOC was estimated using the following equation (Yang et al., 2022):

$$P = \frac{\frac{V}{33.3\%} + \frac{S}{90\%} + C}{10\% \times SOC} \times 100\% \quad (1)$$

where V, S, and C represent the lignin phenol monomers (g kg^{-1}), 10% denotes the general lignin content in the main crops residues (Burgess et al., 2002).

Given that the average conversion values from MurN to bacterial carbon are 45 and GluN to fungal carbon are 9, contributions of microbial residual carbon (MRC) to SOC were calculated based on amino sugar data as follows (Appuhn and Joergensen, 2006; Joergensen, 2018):

$$\text{Bacterial residual C} = 45 \times \text{MurN} \quad (2)$$

$$\text{Fungal residual C} = (\text{GluN}/179.2\text{–}2 \times \text{MurN}/251.2) \times 179.2 \times 9 \quad (3)$$

where 179.2 and 251.2 are the molecular weights of glucosamine and muramic acid, respectively. The total MRC was estimated as the sum of the fungal and bacterial residual carbon.

2.4. Statistical analyses

Data are presented as the mean values and standard errors (n = 3). The significant differences between treatments and between fractions within a treatment were tested using independent two-sample *t*-test at p < 0.05 (SPSS v21.0 software). A principal component analysis (PCA) was performed to evaluate the changes in SOM profiling (molecular composition, source, and degradation) between treatments and fractions (OriginPro 2020 software; OriginLab, Northampton, MA, USA).

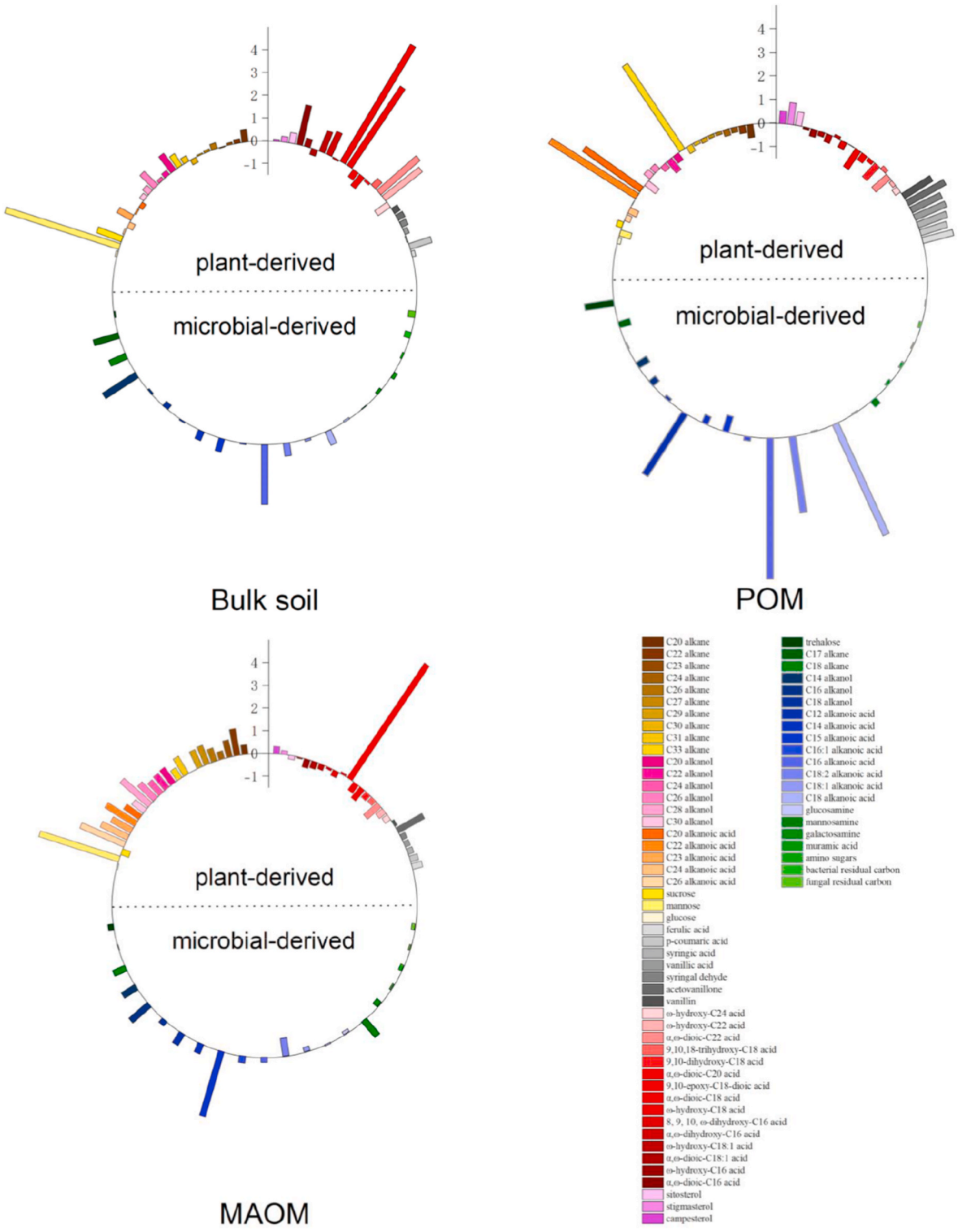

Fig. 2. Response of various extractable biomarkers to mineral fertilizers application compared to the control, of the bulk soil, particulate organic matter (POM), and mineral-associated organic matter (MAOM) fractions. Bars indicate differences in biomarkers concentration between the control and fertilization treatments. Positive values indicate increased concentration and negative values indicate decreased concentration compared to the control.

3. Results

3.1. SOC and TN in bulk soil and fractions

In the non-fertilized treatment, SOC concentrations were 10.2, 3.2, and 12.8 g kg^{-1} in the bulk soil, MAOM, and POM, respectively. After 10 years of fertilization, the SOC concentrations in the fertilized treatment were 11.9, 4.3, and 13.8 g kg^{-1} in the bulk soil, MAOM, and POM fractions, respectively (Table S1). The MAOM fraction dominated the size distribution (>60% of the total recovered mass), and fertilization increased the MAOM mass by 14% (Fig. 1a). Mineral fertilizer addition altered the amounts of SOC (g C kg^{-1} bulk soil) stored in the POM and MAOM fractions, with the majority of SOC being concentrated in the MAOM fraction (approximately 90%). Specifically, fertilization

Table 1
Concentrations of soil organic matter (SOM) components in particulate organic matter (POM) and mineral-associated organic matter (MAOM) fractions from a 10-year field experiment in North China Plain where replicated plots received either no fertilizers or mineral fertilizers.

Compounds name	POM		MAOM	
	Control	Fertilization	Control	Fertilization
Solvent-extracted products (μg g^{-1} soil)				
Short-chain *n*-alkanes (<C_{20})	**0.18 ± 0.02***	0.09 ± 0.01	0.55 ± 0.04	0.90 ± 0.23
Long-chain *n*-alkanes (≥C_{20})	2.11 ± 0.31	1.44 ± 0.17	3.92 ± 0.33	**7.55 ± 0.54***
Short-chain *n*-alkanols	**0.21 ± 0.05***	0.09 ± 0.02	0.72 ± 0.04	1.12 ± 0.19
Long-chain *n*-alkanols	1.16 ± 0.14	0.85 ± 0.07	1.11 ± 0.09	**2.84 ± 0.24***
Short-chain *n*-alkanoic acid	17.8 ± 2.0	17.4 ± 2.3	39.8 ± 2.6	51.5 ± 4.4
Long-chain *n*-alkanoic acid	1.82 ± 0.3	1.29 ± 0.31	1.09 ± 0.06	**2.84 ± 0.48***
Carbohydrate	2.37 ± 0.32	2.14 ± 0.48	2.68 ± 0.14	2.48 ± 0.42
Steroids	1.12 ± 0.15	**2.64 ± 0.21***	2.81 ± 0.15	2.95 ± 0.76
Base hydrolyzed products (μg g^{-1} soil)				
Suberin-derived lipids	**4.30 ± 0.45***	2.08 ± 0.17	**6.07 ± 0.38***	4.25 ± 0.18
Cutin-derived lipids	6.68 ± 1.58	4.83 ± 0.22	10.27 ± 1.06	10.25 ± 1.06
Suberin- or cutin-derived lipids	**8.46 ± 1.69***	4.57 ± 0.3	11.45 ± 0.95	11.87 ± 1.25
Suberin- and cutin-derived lipids	**19.4 ± 3.67***	11.5 ± 0.68	27.8 ± 2.3	26.4 ± 2.1
CuO oxidized products (μg g^{-1} soil)				
Vanillyls	8.85 ± 0.88	**15.76 ± 1.64***	36.65 ± 3.51	**55.4 ± 3.91***
Syringyls	7.00 ± 0.82	**12.00 ± 1.44***	35.06 ± 4.57	48.68 ± 4.35
Cinnamyls	2.19 ± 0.23	**3.67 ± 0.74***	5.2 ± 0.74	**7.99 ± 1.26***
Total lignin-derived phenols	18.0 ± 1.7	**31.4 ± 3.8***	76.9 ± 8.7	**112.1 ± 5.8***
Amino sugars (μg g^{-1} soil)				
Glucosamine	**47.4 ± 0.7***	32.9 ± 5.34	98.5 ± 8.1	95.6 ± 3.8
Mannose	1.41 ± 0.06	1.34 ± 0.15	1.61 ± 0.15	**3.47 ± 0.26***
Galactosamine	**24.4 ± 0.3***	15.7 ± 2.7	34.8 ± 5.0	29.1 ± 0.3
Muramic acid	**3.12 ± 0.06***	1.98 ± 0.31	4.08 ± 0.37	4.26 ± 0.18
Total amino sugars	**76.3 ± 1.0***	51.9 ± 8.4	139.0 ± 13.5	132.5 ± 3.7

Values are presented as means ± SE ($n = 3$). Values that are statistically different between the control and fertilization treatments are indicated by *$p < 0.05$. SOM compound concentrations were normalized to bulk soil dry weight (μg g^{-1} soil).

increased the concentration of SOC by 25% in the MAOM fraction relative to that in the control (Fig. 1b). Fertilization increased the TN concentration in POM by 64% relative to the unfertilized control and decreased the carbon/nitrogen ratio in MAOM and bulk soil (Table S1).

3.2. Free lipids compounds in the POM and MAOM fractions

The free lipids identified in the POM and MAOM fractions and bulk soils are shown in Fig. 2. For the POM fraction, fertilization decreased the concentrations of short-chain *n*-alkanes and *n*-alkanols by 50% and 57%, respectively, but increased plant-derived steroids (i.e., campesterol, stigmasterol, and sitosterol) by 46.4% (Table 1; Fig. 2). Fertilization increased the concentrations of long-chain (≥C_{20}) aliphatic lipids (*n*-alkanes by 93%, *n*-alkanols by 156%, and *n*-alkanoic acids by 161%) in the MAOM fraction, but decreased short-chain (<C_{20}) *n*-alkanes and *n*-alkanols by 50% and 57%, respectively (Table 1). Several molecular indicators were used to assess the source and degradation status of the free lipids (Fig. S1). Overall, ACL_{Alk} and ACL_{Fa} ranged from 26.4 to 27.7 and 16.6–16.9, respectively, across the fractions and treatments (Figs. S1a and c). Compared with the control, the fertilization treatment had a higher ACL_{Alk} in the POM fraction ($p < 0.01$) than in the MAOM fraction (Fig. S1a). Moreover, mineral fertilizer application increased the OEP_{Alk} and EOP_{Fa} in the POM fraction (Figs. S1b and d; $p < 0.001$).

3.3. Bound lipids in the POM and MAOM fractions

Mineral fertilizer application decreased the suberin-derived lipid concentration by 52% in the POM fraction and 30% in the MAOM fraction (Table 1; $p < 0.05$), whereas fertilization did not affect the cutin-derived constituents in both POM and MAOM fractions. The summed cutin- and/or suberin-derived lipids ($\Sigma S^{v}C$; $\Sigma S^{\wedge}C$) were relatively lower under fertilization than the control in the POM fraction rather than the MAOM fraction (Table 1). The addition of mineral fertilizer significantly decreased the suberin/cutin ratio in the POM fraction (Fig. S2a; $p < 0.05$). The ω-$C_{18}/\Sigma C_{18}$ ratio in the POM fraction was higher in the fertilized treatment than that in the control treatment (Fig. S2b; $p < 0.05$). The ω-$C_{16}/\Sigma C_{16}$ ratio in the POM fraction was lower in response to mineral fertilizer addition than that in the unfertilized control (Fig. S2c). In addition, fertilization resulted in a higher $\Sigma mid/\Sigma S^{\wedge}C$ ratio than the control in the POM fraction (Fig. S2d).

3.4. Lignin-derived phenols in the POM and MAOM fractions

Mineral fertilizer application increased the specific and total lignin-derived phenols in both POM and MAOM fractions (Fig. 2; Table 1). Specifically, fertilized (cf. control) treatment increased the total lignin-derived phenol concentrations by 74% and 31% in the POM and MAOM fractions, respectively (Fig. 2; Table 1). The lignin oxidation ratios, expressed as $(Ad/Al)_V$ and $(Ad/Al)_S$, were similar between the two fertilizer regimes (Fig. S3). However, the POM fraction demonstrated a higher $(Ad/Al)_V$ value than the MAOM fraction within specific treatment, whereas the reverse trend was found for the $(Ad/Al)_S$ ratio between the POM and MAOM fractions (Fig. S3).

3.5. Amino sugars and microbial necromass in the POM and MAOM fractions

Mineral fertilizers application altered the specific amino sugars (e.g., glucosamine, mannosamine, galactosamine, and muramic acid) between the soil fractions (Fig. 2; Table 1). Fertilization reduced some amino sugars (except mannosamine) and total amino sugars by 31–37% ($p < 0.05$), whereas the changes in these specific and total amino sugars were not significant in the MAOM fraction. We also observed that the changes in fungal and bacterial MRC in the two soil fractions (Fig. 3). Specifically, mineral fertilizer application decreased bacterial MRC by 37% in the POM fraction, whereas MRC in the MAOM fraction was not significant between the treatments. Fertilization decreased the bacterial MRC and its contribution to SOC in the POM fraction (Fig. 3a and d), and similar trend was observed in the contributions of fungal MRC and total MRC to SOC in the MAOM fraction (Fig. 3e and f). Across the treatments, the POM fraction demonstrated higher ratios of bacterial MRC, fungal MRC and total MRC to SOC than those in the MAOM fraction (Fig. 3d–f). Furthermore, mineral fertilizer resulted in a higher bacterial MRC in the MAOM fraction than that in the POM fraction (Fig. 3a). Similarly, a higher fungal MRC was observed in the MAOM fraction than in the POM fraction across treatments, despite insignificant changes between treatments (Fig. 3b). Fertilization decreased the bacterial-to-fungal MRC ratio (B/F) in the POM fraction rather than in the MAOM fraction (Fig. 3c), whereas this ratio was higher in POM than MAOM fraction across the treatments.

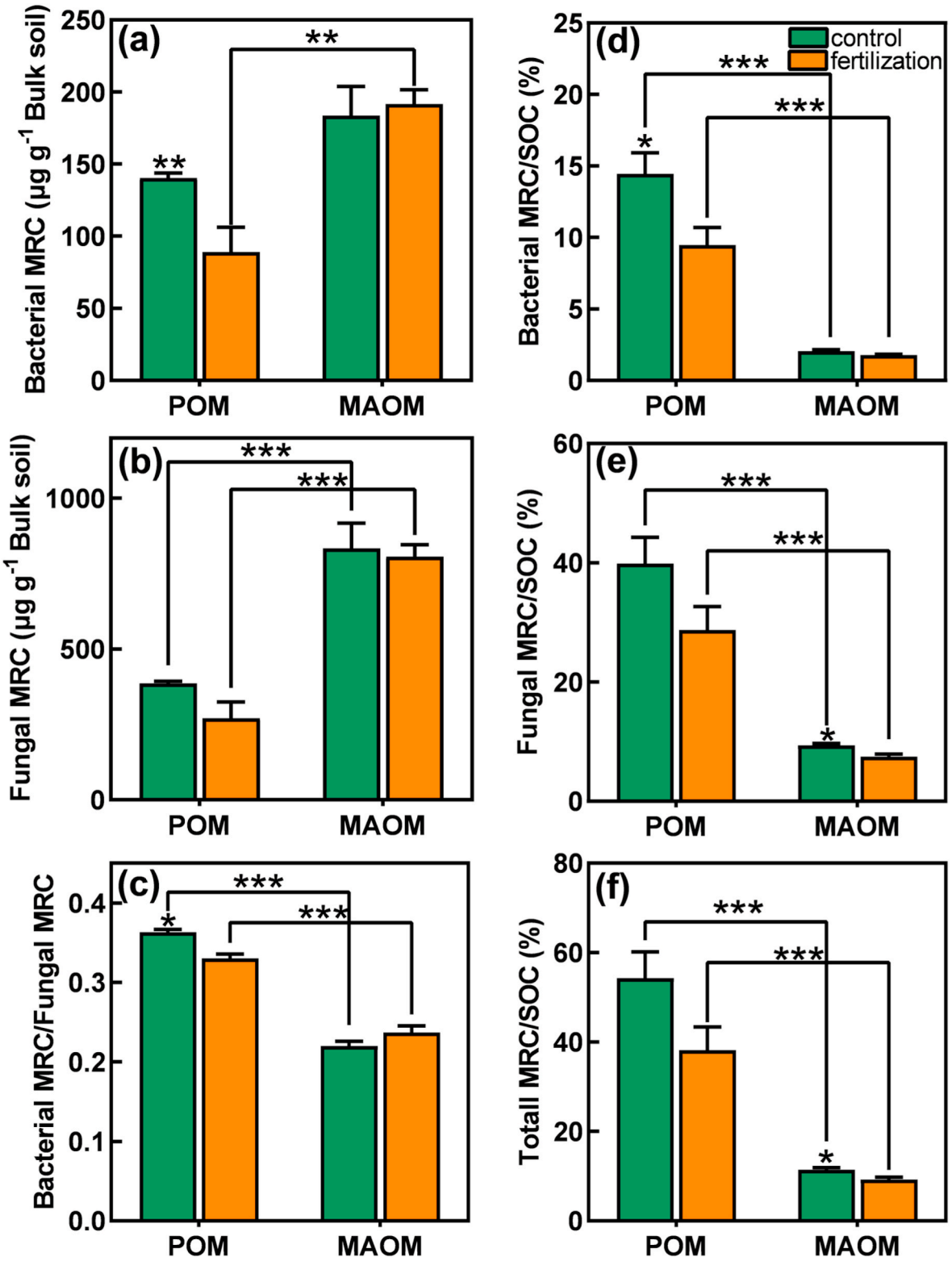

Fig. 3. Response of bacterial, fungal, and their microbial residual carbon (MRC) contribution to soil organic carbon (SOC) accumulation in the particulate organic matter (POM) and mineral-associated organic matter (MAOM) fractions as influenced by mineral fertilizer application. Values represent means ± SE ($n = 3$) for the control and fertilization treatments. *$p < 0.05$, **$p < 0.01$, and ***$p < 0.001$.

3.6. SOM compounds and proxies in the POM and MAOM fractions

Using the molecular components and related proxies analyzed above, changes in SOM status with fertilization in the POM and MAOM fractions were evaluated using principal component analysis (Fig. 4). The resultant principal components (PCs) explained 78.7% of the variance, and both treatments were separated from one another along PC1, whereas both fractions were separated from one another along PC2 (Fig. 4). B/F, $(Ad/Al)_V$, ω-$C_{18}/\Sigma C_{18}$, and ACL_{Fa} had higher negative loading scores, while EOP_{Fa}, ACL_{Fa}, ω-$C_{16}/\Sigma C_{16}$, ω-$C_{18}/\Sigma C_{18}$, and

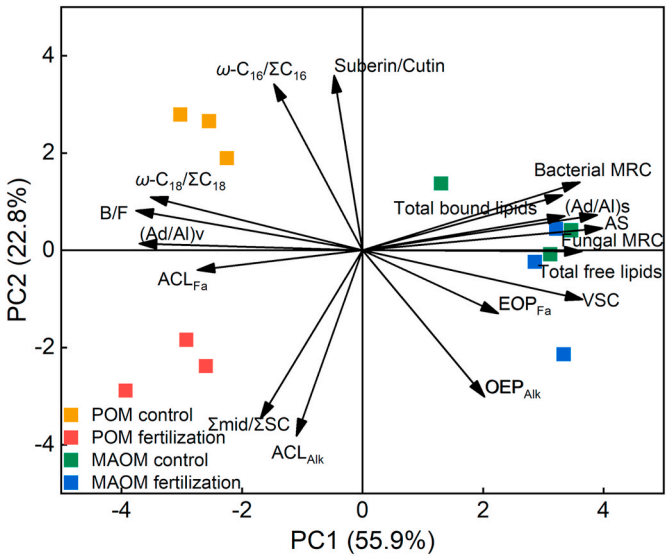

Fig. 4. Biplots of principal component analysis (PCA) between compounds and related degradation proxies. Numbers in parenthesis represent data variations explained by first two principal components (PCs). ACL_{Alk}: average chain length of *n*-alkanes; ACL_{Fa}: average chain length of *n*-alkanoic acids; OEP_{Alk}: odd-over-even predominance of *n*-alkanes; EOP_{Fa}: even-over-odd predominance of *n*-alkanoic acids; ω-$C_{16}/\Sigma C_{16}$: C_{16} ω-hydroxy-alkanoic acids to all hydrolysable C_{16} aliphatic lipids; ω-$C_{18}/\Sigma C_{18}$: C_{18} ω-hydroxy-alkanoic acids to all hydrolysable C_{18} aliphatic lipids; Σmid/ΣS^C: the ratio of mid-chain-substituted hydroxy and epoxy acids to total cutin- and suberin-derived compounds; $(Ad/Al)_S$: the ratio of acid to aldehyde for syringyls; $(Ad/Al)_V$: the ratio of acid to aldehyde for vanillyls; VSC: total lignin-derived phenols; AS: total amino sugars; Fungal MRC: fungal microbial residual carbon; Bacterial MRC: bacterial microbial residual carbon.

suberin/cutin had higher positive loading scores along PC1. The control treatment was distinguished by ω-$C_{16}/\Sigma C_{16}$ and ω-$C_{18}/\Sigma C_{18}$, whereas fertilized treatment was distinguished by Σmid/ΣS^C and ACL_{Alk} in the POM fraction. In contrast, in the MAOM fraction, the control treatment was shaped by total amino sugars (AS), bacterial MRC, and total bound lipids, whereas fertilized treatment was shaped by total lignin-derived phenols (VSC), total free lipids, EOP_{Fa}, and OEP_{Alk}. The resultant PCs explained 74.6% and 66.1% of the variance in the POM and MAOM fractions, respectively (Fig. S4). After decadal fertilization, the contribution of plant-derived carbon to SOC increased from 38% to 52% in POM and from 17% to 21% in MAOM, whereas the contribution of microbial-derived carbon to SOC decreased from 54% to 38% in POM and 11%–9% in MAOM (Fig. 5).

4. Discussion

4.1. Effect of mineral fertilizers on SOM origins in the POM and MAOM fractions

Overall, our results showed that decadal fertilization significantly altered the molecular composition and origins of SOC rather than its concentration (Fig. 1; Table 1). The lack of significant changes in SOC concentrations with mineral fertilizers may be attributed to the balance between carbon inputs and degradation (Man et al., 2021). This may also be because SOC accrual in response to fertilization needs decades or longer to manifest (Wiesmeier et al., 2019; Xu et al., 2021). Despite similar SOC concentrations in bulk soil, the application of mineral fertilizer elevated the SOC amount by 26% in the MAOM fraction, implying enhanced carbon persistence (Kleber et al., 2015).

We found a higher proportion of plant-derived carbon (29–32% of SOC in bulk soils) and a lower proportion of microbial-derived carbon (13–20% of SOC) (Fig. 5), which is consistent with a previous study using the same methodology (Chen et al., 2021). However, some previous reports have estimated that MRC contributes over 50% to SOC in temperate cropland soil (Liang et al., 2019; Angst et al., 2021; Wang et al., 2021), which is generally higher than that in the current study. This is because soil pH has a negative effect on amino sugars accumulation (Ni et al., 2020), and the alkaline soil conditions in this study (Table S1) may be the reason for the lower contribution of MRC to SOC.

Our results showed that mineral fertilizer application increased the contribution of plant-derived carbon to SOC in bulk soils (32% vs. 29%) but decreased the microbial-derived contribution (13% vs. 20%) (Fig. 5). This may be attributed to higher crop carbon inputs after fertilization (He et al., 2018). Furthermore, fertilization has been shown to weaken microbial anabolism and necromass accumulation (Janssens et al., 2010). Regarding the fractions, we observed a much higher contribution of plant-derived carbon in the POM than in the MAOM fraction (Fig. 5). This suggests that POM acts as a functional hot-spot

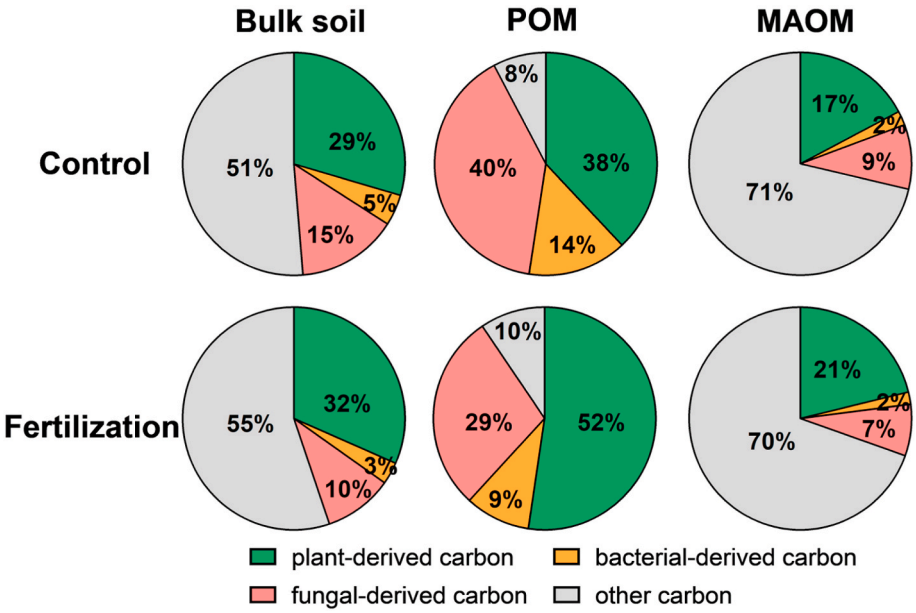

Fig. 5. Contributions of plant- (quantified as lignin), bacterial-, and fungal-derived carbon to soil organic carbon (SOC) in corresponding fractions.

where large amounts of plant-derived organic matter are transformed into SOM by microorganisms (Witzgall et al., 2021). The contribution of microbial residues to SOC in the MAOM fraction was lower than that in the POM fraction, which could be explained by the dilution effect from the incorporation of other SOC components in the MAOM fraction, resulting in higher amounts of SOC than the POM fraction (Fig. 1b). Moreover, PCA further verified that the POM and MAOM fractions differed in their composition (Fig. 4).

4.2. Different response of free lipids, bound lipids, and lignin-derived phenols to mineral fertilizers

Fertilization increased plant-derived steroids in the POM fraction (Fig. 2; Table 1), which is in line with previous studies that reported that nitrogen addition selectively preserved steroids from cropland (Man et al., 2021). The elevated levels of steroids after fertilization may originate from crop residue input. This coincided with the higher contribution of plant-derived carbon under fertilization in the POM fraction (Fig. 5). Thus, as a characteristic of fresh plant material, higher OEP_{Alk} values in the POM fraction in fertilized soils (Fig. S1b) further supported this inference (Schäfer et al., 2016). When fresh crop residues enter the POM fraction, labile components such as short-chain lipids may be decomposed faster in the fertilized treatment (Miller et al., 2019; Jilling et al., 2020; Thomas et al., 2021), as evidenced by the higher ACL_{Alk} in the POM fraction under fertilized soils (Fig. S1a). In contrast, fertilization selectively preserved long-chain lipids in the MAOM fraction (Table 1), probably because of their recalcitrance and affinity with mineral surfaces to form mineral-organic associations (Wiesenberg et al., 2010). The inconsistent responses of short- and long-chain aliphatic lipids in the POM and MAOM fractions indicate that mineral fertilizers may stimulate the preferential degradation of specific free lipid components (e.g., $<C_{20}$ *n*-alkanes and *n*-alkanols), leading to the relative enrichment of long-chain lipids in the MAOM fraction (Table 1).

The present study showed that fertilization reduced the suberin-derived compounds relative to the control (Table 1), reflecting lower root-derived carbon accrual in the fertilized soil. This result supports the argument that less crop carbon is allocated to root growth under higher soil nutrient availability (Li et al., 2015). The lower suberin/cutin ratio in the fertilized treatment (Fig. S2a) implies that fertilization preferentially promoted aboveground growth relative to belowground (Lu et al., 2011). The reduced ω-$C_{16}/\Sigma C_{16}$ ratio under fertilization in the POM fraction (Fig. S2c) indicated inhibited degradation of cutin-derived compounds under fertilization. Interestingly, the application of mineral fertilizers suppressed cutin-derived compounds degradation in POM, but not in the MAOM fraction (Fig. S2), indicating that the POM fraction is more susceptible to nutrient management than the MAOM fraction (Miller et al., 2019; Jilling et al., 2020).

Mineral fertilizers application increased lignin-derived phenols in both POM and MAOM fractions (Fig. 2; Table 1), which was likely due to the increasing straw input (Liu et al., 2016). Lignin distribution in soils is the result of input and decomposition processes (Thevenot et al., 2010). In the present study, lignin degradation proxies, as assessed by $(Ad/Al)_V$ and $(Ad/Al)_S$, were not affected by the application of mineral fertilizers (Fig. S3). This further indicated that the elevated lignin-derived phenols resulted from the added crop residue inputs in the cropland. Regarding the soil fractions, MAOM presented higher $(Ad/Al)_S$ ratio than the POM fraction across treatments, indicating higher degradation of syringyls monomers in MAOM (Fig. S3a). However, we observed the opposite pattern for (Ad/Al)v between the POM and MAOM fractions (Fig. S3b). It is likely that vanillyls monomers are more recalcitrant than syringyls monomers during decomposition (Hedges et al., 1988; Bahri et al., 2006). Thus, the vanillyls monomers have a higher probability of interacting with mineral surfaces to form mineral-associated complexity and aggregate (Clemente et al., 2012).

4.3. Different response of microbial residues to mineral fertilizers

Mineral fertilizer application significantly decreased the individual and total amino sugars and MRC in both POM and MAOM fractions (Table 1; Fig. 3), which is consistent with other reports in cropland (Chen et al., 2020), grassland, and forest ecosystems (Liang and Balser, 2012; Yuan et al., 2020). Lower microbial residues in fertilized treatments indicate that microbes tend to invest less carbon in anabolism during fertilization (Spohn et al., 2016). Microbial necromass accumulates continuously through the formation of microbial biomass and stabilization of its residues and is gradually consumed through mineralization (Schimel and Schaeffer, 2012; Liang et al., 2019). The decreased contribution of microbial residues to SOC may be associated with enhanced microbial necromass decomposition in response to fertilization (Wang et al., 2021). Although amino sugars play a crucial role in SOM formation, they can be utilized as energy sources (e.g., carbon and nitrogen) to feed microbial growth and activities (Wang et al., 2021). Indeed, long-term N fertilization caused carbon limitation in the soil (Chen et al., 2018), as evidenced by the lower SOC/TN ratio in our study (Table S1). This may result in higher decomposition of microbial necromass as energy to compensate for the microbial carbon demand (Cui et al., 2020; Wang et al., 2021). The additional phosphate fertilizer could promote microbial carbon acquisition by increasing the activity of β-N-acetyl-glucosaminidase and thus microbial residues decomposition (Sinsabaugh et al., 2008; Yuan et al., 2020).

Mineral fertilizers application lowered the B/F ratio in the POM fraction (Fig. 3c), implying that bacterial residues had a relatively faster turnover rate than fungal residues (He et al., 2011). In addition, microbes prefer to use labile substrates enriched in POM form (Cui et al., 2020; Witzgall et al., 2021), resulting in lower bacterial residues due to less protection (Fig. 3a and d). However, bacterial cells can attach directly to clay surfaces non-specifically (Olivelli et al., 2020), which resulted in insignificant differences in bacterial MRC and the contribution of bacterial MRC to SOC within the MAOM fraction. In the present study, higher amino sugars, fungal MRC, and bacterial MRC were observed in the MAOM fraction than in POM (Fig. 3; $p < 0.05$). Likely, due to high affinity for mineral surfaces, microbial necromass may be entrapped into the MAOM fraction, leading to less accessibility by soil enzymes. (Angst et al., 2021).

5. Conclusion

The current study found that a 10-year period fertilization altered the molecular composition of SOM rather than its quantity. Furthermore, it provided detailed information on the composition and origins of SOM related to its stabilization and persistence and highlighted the different responses of plant-derived carbon and MRC to mineral fertilizers in the contrasting POM and MAOM fractions. Collectively, the results suggest that mineral fertilizers increase the size of the MAOM-associated carbon pools, by increasing stable components, which enhances SOC sequestration and its persistence in temperate agroecosystems.

Declaration of competing interest

The authors declare that they have no known competing financial interests or personal relationships that could have appeared to influence the work reported in this paper.

Data availability

Data will be made available on request.

Acknowledgements

This study was financially supported by the Natural Science Foundation of China (41671305; 42077037) and the National Key Research

& Development Program of China (2022YFD1901100). Zhangliu Du thanks Myrna J. Simpson at the University of Toronto Scarborough for training the biomarker soil extraction and processing. Davey Jones was supported by the UKRI Natural Environment Research Council GCRF project NE/V005871/1.

Appendix A. Supplementary data

Supplementary data to this article can be found online at https://doi.org/10.1016/j.soilbio.2023.109042.

References

Amelung, W., Bossio, D., de Vries, W., Kögel-Knabner, I., Lehmann, J., Amundson, R., Bol, R., Collins, C., Lal, R., Leifeld, J., 2020. Towards a global-scale soil climate mitigation strategy. Nature Communications 11, 1–10.

Amelung, W., Brodowski, S., Sandhage-Hofmann, A., Bol, R., 2008. Combining biomarker with stable isotope analyses for assessing the transformation and turnover of soil organic matter. Advances in Agronomy 100, 155–250.

Angst, G., Mueller, K.E., Nierop, K., Simpson, M.J., 2021. Plant-or microbial-derived? A review on the molecular composition of stabilized soil organic matter. Soil Biology and Biochemistry 156, 108189.

Appuhn, A., Joergensen, R.G., 2006. Microbial colonisation of roots as a function of plant species. Soil Biology and Biochemistry 38, 1040–1051.

Averill, C., Waring, B., 2018. Nitrogen limitation of decomposition and decay: how can it occur? Global Change Biology 24, 1417–1427.

Bahri, H., Dignac, M.F., Rumpel, C., Rasse, D.P., Chenu, C., Mariotti, A., 2006. Lignin turnover kinetics in an agricultural soil is monomer specific. Soil Biology and Biochemistry 38, 1977–1988.

Bergen, P., Nott, C.J., Bull, I.D., Poulton, P.R., Evershed, R.P., 1998. Organic geochemical studies of soils from the Rothamsted Classical Experiments - IV. Preliminary results from a study of the effect of soil pH on organic matter decay. Organic Geochemistry 29, 1779–1795.

Boot, C.M., Hall, E.K., Denef, K., Baron, J.S., 2016. Long-term reactive nitrogen loading alters soil carbon and microbial community properties in a subalpine forest ecosystem. Soil Biology and Biochemistry 92, 211–220.

Brown, R.W., Chadwick, D.R., Bending, G.D., Collins, C.D., Whelton, H.L., Daulton, E., Covington, J.A., Bull, I.D., Jones, D.L., 2022. Nutrient (C, N and P) enrichment induces significant changes in the soil metabolite profile and microbial carbon partitioning. Soil Biology and Biochemistry 172, 108779.

Burgess, M., Mehuys, G., Madramootoo, C., 2002. Decomposition of grain-corn residues (Zea mays L.): a litterbag study under three tillage systems. Canadian Journal of Soil Science 82, 127–138.

Cambardella, C.A., Elliott, E.T., 1992. Particulate soil organic-matter changes across a grassland cultivation sequence. Soil Science Society of America Journal 56, 777–783.

Cassman, K.G., Dobermann, A., 2022. Nitrogen and the future of agriculture: 20 years on. Ambio 51, 17–24.

Chassé, M., Lutfalla, S., Cecillon, L., Baudin, F., Abiven, S., Chenu, C., Barré, P., 2021. Long-term bare-fallow soil fractions reveal thermo-chemical properties controlling soil organic carbon dynamics. Biogeochemistry 18, 1703–1718.

Chen, H., Li, D., Zhao, J., Zhang, W., Xiao, K., Wang, K., 2018. Nitrogen addition aggravates microbial carbon limitation: evidence from ecoenzymatic stoichiometry. Geoderma 329, 61–64.

Chen, X., Han, X., Yan, J., Lu, X., Hao, X., Wang, W., Biswas, A., Zhu-Barker, X., Zou, W., 2020. Land use and mineral fertilization influence soil microbial biomass and residues: a case study of a Chinese Mollisol. European Journal of Soil Biology 100, 103216.

Chen, X., Hu, Y., Xia, Y., Zheng, S., Ma, C., Rui, Y., He, H., Huang, D., Zhang, Z., Ge, T., 2021. Contrasting pathways of carbon sequestration in paddy and upland soils. Global Change Biology 27, 2478–2490.

Chenu, C., Angers, D.A., Barré, P., Derrien, D., Arrouays, D., Balesdent, J., 2019. Increasing organic stocks in agricultural soils: knowledge gaps and potential innovations. Soil and Tillage Research 188, 41–52.

Clemente, J.S., Simpson, A.J., Simpson, M.J., 2012. Association of specific organic matter compounds in size fractions of soils under different environmental controls. Organic Geochemistry 42, 1169–1180.

Cotrufo, M.F., Ranalli, M.G., Haddix, M.L., Six, J., Lugato, E., 2019. Soil carbon storage informed by particulate and mineral-associated organic matter. Nature Geoscience 12, 989–994.

Cotrufo, M.F., Soong, J.L., Horton, A.J., Campbell, E.E., Haddix, M.L., Wall, D.H., Parton, W.J., 2015. Formation of soil organic matter via biochemical and physical pathways of litter mass loss. Nature Geoscience 8, 776–779.

Creme, A., Chabbi, A., Gastal, F., Rumpel, C., 2017. Biogeochemical nature of grassland soil organic matter under plant communities with two nitrogen sources. Plant and Soil 415, 189–201.

Creme, A., Rumpel, C., Le Roux, X., Romian, A., Lan, T., Chabbi, A., 2018. Ley grassland under temperate climate had a legacy effect on soil organic matter quantity, biogeochemical signature and microbial activities. Soil Biology and Biochemistry 122, 203–210.

Cui, J., Zhu, Z., Xu, X., Liu, S., Jones, D.L., Kuzyakov, Y., Shibistova, O., Wu, J., Ge, T., 2020. Carbon and nitrogen recycling from microbial necromass to cope with C: N stoichiometric imbalance by priming. Soil Biology and Biochemistry 142, 107720.

Dou, X., He, P., Zhu, P., Zhou, W., 2016. Soil organic carbon dynamics under long-term fertilization in a black soil of China: evidence from stable C isotopes. Scientific Reports 6, 1–10.

Fan, Y., Yang, L., Zhong, X., Yang, Z., Lin, Y., Guo, J., Chen, G., Yang, Y., 2020. N addition increased microbial residual carbon by altering soil P availability and microbial composition in a subtropical Castanopsis forest. Geoderma 375, 114470.

Feng, X., Simpson, A.J., Schlesinger, W.H., Simpson, M.J., 2010. Altered microbial community structure and organic matter composition under elevated CO2 and N fertilization in the duke forest. Global Change Biology 16, 2104–2116.

Feng, X., Simpson, M.J., 2007. The distribution and degradation of biomarkers in Alberta grassland soil profiles. Organic Geochemistry 38, 1558–1570.

Gao, Q., Ma, L., Fang, Y., Zhang, A., Li, G., Wang, J., Wu, D., Wu, W., Du, Z., 2021. Conservation tillage for 17 years alters the molecular composition of organic matter in soil profile. Science of the Total Environment 762, 143116.

Ge, Z., Li, S., Bol, R., Zhu, P., Peng, C., An, T., Cheng, N., Liu, X., Li, T., Xu, Z., 2021. Differential long-term fertilization alters residue-derived labile organic carbon fractions and microbial community during straw residue decomposition. Soil and Tillage Research 213, 105120.

Hamer, U., Rumpel, C., Dignac, M.F., 2012. Cutin and suberin biomarkers as tracers for the turnover of shoot and root derived organic matter along a chronosequence of Ecuadorian pasture soils. European Journal of Soil Science 63, 808–820.

He, H., Zhang, W., Zhang, X., Xie, H., Zhuang, J., 2011. Temporal responses of soil microorganisms to substrate addition as indicated by amino sugar differentiation. Soil Biology and Biochemistry 43, 1155–1161.

He, R., Shao, C., Shi, R., Zhang, Z., Zhao, R., 2020. Development trend and driving factors of agricultural chemical fertilizer efficiency in China. Sustainability 12, 4607.

He, Y., He, X., Xu, M., Zhang, W., Yang, X., Huang, S., 2018. Long-term fertilization increases soil organic carbon and alters its chemical composition in three wheat-maize cropping sites across central and south China. Soil and Tillage Research 177, 79–87.

Hedges, J.I., Blanchette, R.A., Weliky, K., Devol, A.H., 1988. Effects of fungal degradation on the CuO oxidation products of lignin: a controlled laboratory study. Geochimica et Cosmochimica Acta 52, 2717–2726.

Hemingway, J.D., Rothman, D.H., Grant, K.E., Rosengard, S.Z., Eglinton, T.I., Derry, L.A., Galy, V., 2019. Mineral protection regulates long-term global preservation of natural organic carbon. Nature 570, 228–231.

Hoffland, E., Kuyper, T.W., Comans, R.N., Creamer, R.E., 2020. Eco-functionality of organic matter in soils. Plant and Soil 455, 1–22.

Hu, J., Huang, C., Zhou, S., Liu, X., Dijkstra, F.A., 2022. Nitrogen addition increases microbial necromass in croplands and bacterial necromass in forests: a global meta-analysis. Soil Biology and Biochemistry 165, 108500.

Janssens, I., Dieleman, W., Luyssaert, S., Subke, J.-A., Reichstein, M., Ceulemans, R., Ciais, P., Dolman, A.J., Grace, J., Matteucci, G., 2010. Reduction of forest soil respiration in response to nitrogen deposition. Nature Geoscience 3, 315–322.

Jilling, A., Kane, D., Williams, A., Yannarell, A.C., Davis, A., Jordan, N.R., Koide, R.T., Mortensen, D.A., Smith, R.G., Snapp, S.S., 2020. Rapid and distinct responses of particulate and mineral-associated organic nitrogen to conservation tillage and cover crops. Geoderma 359, 114001.

Joergensen, R.G., 2018. Amino sugars as specific indices for fungal and bacterial residues in soil. Biology and Fertility of Soils 54, 559–568.

Kaiser, M., Ellerbrock, R., 2005. Functional characterization of soil organic matter fractions different in solubility originating from a long-term field experiment. Geoderma 127, 196–206.

Kauer, K., Pärnpuu, S., Talgre, L., Eremeev, V., Luik, A., 2021. Soil particulate and mineral-associated organic matter increases in organic farming under cover cropping and manure addition. Agriculture 11, 903.

Khan, S., Mulvaney, R., Ellsworth, T., Boast, C., 2007. The myth of nitrogen fertilization for soil carbon sequestration. Journal of Environmental Quality 36, 1821–1832.

Kleber, M., Eusterhues, K., Keiluweit, M., Mikutta, C., Mikutta, R., Nico, P.S., 2015. Mineral–organic associations: formation, properties, and relevance in soil environments. Advances in Agronomy 130, 1–140.

Kögel-Knabner, I., 2002. The macromolecular organic composition of plant and microbial residues as inputs to soil organic matter. Soil Biology and Biochemistry 34, 139–162.

Kopittke, P.M., Berhe, A.A., Carrillo, Y., Cavagnaro, T.R., Chen, D., Chen, Q.-L., Roman Dobarco, M., Dijkstra, F.A., Field, D.J., Grundy, M.J., 2022. Ensuring planetary survival: the centrality of organic carbon in balancing the multifunctional nature of soils. Critical Reviews in Environmental Science and Technology 52, 4308–4324.

Ladha, J.K., Reddy, C.K., Padre, A.T., van Kessel, C., 2011. Role of nitrogen fertilization in sustaining organic matter in cultivated soils. Journal of Environmental Quality 40, 1756–1766.

Lavallee, J.M., Soong, J.L., Cotrufo, M.F., 2020. Conceptualizing soil organic matter into particulate and mineral-associated forms to address global change in the 21st century. Global Change Biology 26, 1–13.

Lehmann, J., Kleber, M., 2015. The contentious nature of soil organic matter. Nature 528, 60–68.

Li, W., Jin, C., Guan, D., Wang, Q., Wang, A., Yuan, F., Wu, J., 2015. The effects of simulated nitrogen deposition on plant root traits: a meta-analysis. Soil Biology and Biochemistry 82, 112–118.

Liang, C., Amelung, W., Lehmann, J., Kästner, M., 2019. Quantitative assessment of microbial necromass contribution to soil organic matter. Global Change Biology 25, 3578–3590.

Liang, C., Balser, T.C., 2012. Warming and nitrogen deposition lessen microbial residue contribution to soil carbon pool. Nature Communications 3, 1–4.
Liang, C., Schimel, J.P., Jastrow, J.D., 2017. The importance of anabolism in microbial control over soil carbon storage. Nature Microbiology 2, 17105.
Liu, J., Wu, N., Wang, H., Sun, J., Peng, B., Jiang, P., Bai, E., 2016. Nitrogen addition affects chemical compositions of plant tissues, litter and soil organic matter. Ecology 97, 1796–1806.
Lu, M., Zhou, X., Luo, Y., Yang, Y., Fang, C., Chen, J., Li, B., 2011. Minor stimulation of soil carbon storage by nitrogen addition: a meta-analysis. Agriculture, Ecosystems & Environment 140, 234–244.
Ludwig, M., Achtenhagen, J., Miltner, A., Eckhardt, K.-U., Leinweber, P., Emmerling, C., Thiele-Bruhn, S., 2015. Microbial contribution to SOM quantity and quality in density fractions of temperate arable soils. Soil Biology and Biochemistry 81, 311–322.
Ma, L., Ju, Z., Fang, Y., Vancov, T., Gao, Q., Wu, D., Zhang, A., Wang, Y., Hu, C., Wu, W., 2022a. Soil warming and nitrogen addition facilitates lignin and microbial residues accrual in temperate agroecosystems. Soil Biology and Biochemistry 170, 108693.
Ma, S., Chen, G., Du, E., Tian, D., Xing, A., Shen, H., Ji, C., Zheng, C., Zhu, J., Zhu, J., 2021. Effects of nitrogen addition on microbial residues and their contribution to soil organic carbon in China's forests from tropical to boreal zone. Environmental Pollution 268, 115941.
Ma, X., Zhang, W., Zhang, X., Bao, X., Xie, H., Li, J., He, H., Liang, C., Zhang, X., 2022b. Dynamics of microbial necromass in response to reduced fertilizer application mediated by crop residue return. Soil Biology and Biochemistry 165, 108512.
Man, M., Deen, B., Dunfield, K.E., Wagner-Riddle, C., Simpson, M.J., 2021. Altered soil organic matter composition and degradation after a decade of nitrogen fertilization in a temperate agroecosystem. Agriculture, Ecosystems Environmental 310, 107305.
Miller, G., Rees, R., Griffiths, B., Ball, B., Cloy, J., 2019. The sensitivity of soil organic carbon pools to land management varies depending on former tillage practices. Soil and Tillage Research 194, 104299.
Ni, H., Liu, C., Sun, B., Liang, Y., 2022. Response of global farmland soil organic carbon to nitrogen application over time depends on soil type. Geoderma 406, 115542.
Ni, X., Liao, S., Tan, S., Wang, D., Yang, Y., 2020. A quantitative assessment of amino sugars in soil profiles. Soil Biology and Biochemistry 143, 107762.
Nierop, K.G.J., Naafs, D.F.W., Verstraten, J.M., 2003. Occurrence and distribution of ester-bound lipids in Dutch coastal dune soils along a pH gradient. Organic Geochemistry 34, 719–729.
Olivelli, M.S., Fugariu, I., Torres Sanchez, R.M., Curutchet, G., Simpson, A.J., Simpson, M.J., 2020. Unraveling mechanisms behind biomass–clay interactions using comprehensive multiphase nuclear magnetic resonance (NMR) spectroscopy. ACS Earth Space Chemistry 4, 2061–2072.
Otto, A., Shunthirasingham, C., Simpson, M.J., 2005. A comparison of plant and microbial biomarkers in grassland soils from the Prairie Ecozone of Canada. Organic Geochemistry 36, 425–448.
Otto, A., Simpson, M.J., 2006a. Evaluation of CuO oxidation parameters for determining the source and stage of lignin degradation in soil. Biogeochemistry 80, 121–142.
Otto, A., Simpson, M.J., 2006b. Sources and composition of hydrolysable aliphatic lipids and phenols in soils from western Canada. Organic Geochemistry 37, 385–407.
Samson, M.L., Chantigny, M.H., Vanasse, A., Menasseri-Aubry, S., Angers, D.A., 2020. Management practices differently affect particulate and mineral-associated organic matter and their precursors in arable soils. Soil Biology and Biochemistry 148, 107867.
Schäfer, I.K., Lanny, V., Franke, J., Eglinton, T.I., Zech, M., Vysloužilová, B., Zech, R., 2016. Leaf waxes in litter and topsoils along a European transect. Soils 2, 551–564.
Schimel, J.P., Schaeffer, S.M., 2012. Microbial control over carbon cycling in soil. Frontiers in Microbiology 3, 348.
Singh, P., Benbi, D.K., 2018. Nutrient management effects on organic carbon pools in a sandy loam soil under rice-wheat cropping. Archives of Agronomy and Soil Science 64, 1879–1891.
Sinsabaugh, R.L., Lauber, C.L., Weintraub, M.N., Ahmed, B., Allison, S.D., Crenshaw, C., Contosta, A.R., Cusack, D., Frey, S., Gallo, M.E., 2008. Stoichiometry of soil enzyme activity at global scale. Ecology Letters 11, 1252–1264.
Six, J., Paustian, K., 2014. Aggregate-associated soil organic matter as an ecosystem property and a measurement tool. Soil Biology and Biochemistry 68, A4–A9.
Sokol, N.W., Sanderman, J., Bradford, M.A., 2019. Pathways of mineral-associated soil organic matter formation: integrating the role of plant carbon source, chemistry, and point of entry. Global Change Biology 25, 12–24.
Song, J., Wan, S., Piao, S., Knapp, A.K., Classen, A.T., Vicca, S., Ciais, P., Hovenden, M.J., Leuzinger, S., Beier, C., 2019. A meta-analysis of 1,119 manipulative experiments on terrestrial carbon-cycling responses to global change. Nature Ecology Evolution 3, 1309–1320.
Spohn, M., Pötsch, E.M., Eichorst, S.A., Woebken, D., Wanek, W., Richter, A., 2016. Soil microbial carbon use efficiency and biomass turnover in a long-term fertilization experiment in a temperate grassland. Soil Biology and Biochemistry 97, 168–175.
Thevenot, M., Dignac, M.F., Rumpel, C., 2010. Fate of lignins in soils: a review. Soil Biology and Biochemistry 42, 1200–1211.
Thomas, C.L., Jansen, B., van Loon, E.E., Wiesenberg, G.L., 2021. Transformation of n-alkanes from plant to soil: a review. Soils 7, 785–809.
Treseder, K.K., 2008. Nitrogen additions and microbial biomass: a meta-analysis of ecosystem studies. Ecology Letters 11, 1111–1120.
Vandenenden, L., Anthony, M.A., Frey, S., Simpson, M.J., 2021. Biogeochemical evolution of soil organic matter composition after a decade of warming and nitrogen addition. Biogeochemistry 156, 161–175.
Vandenenden, L., Frey, S.D., Nadelhoffer, K.J., Lemoine, J.M., Lajtha, K., Simpson, M.J., 2018. Molecular-level changes in soil organic matter composition after 10 years of litter, root and nitrogen manipulation in a temperate forest. Biogeochemistry 141, 183–197.
Wang, B., An, S., Liang, C., Liu, Y., Kuzyakov, Y., 2021. Microbial necromass as the source of soil organic carbon in global ecosystems. Soil Biology and Biochemistry 162, 108422.
Wang, J.J., Bowden, R.D., Lajtha, K., Washko, S.E., Wurzbacher, S.J., Simpson, M.J., 2019. Long-term nitrogen addition suppresses microbial degradation, enhances soil carbon storage, and alters the molecular composition of soil organic matter. Biogeochemistry 142, 299–313.
Wiesenberg, G.L.B., Dorodnikov, M., Kuzyakov, Y., 2010. Source determination of lipids in bulk soil and soil density fractions after four years of wheat cropping. Geoderma 156, 267–277.
Wiesmeier, M., Urbanski, L., Hobley, E., Lang, B., von Lützow, M., Marin-Spiotta, E., van Wesemael, B., Rabot, E., Ließ, M., Garcia-Franco, N., 2019. Soil organic carbon storage as a key function of soils-A review of drivers and indicators at various scales. Geoderma 333, 149–162.
Witzgall, K., Vidal, A., Schubert, D.I., Höschen, C., Schweizer, S.A., Buegger, F., Pouteau, V., Chenu, C., Mueller, C.W., 2021. Particulate organic matter as a functional soil component for persistent soil organic carbon. Nature Communications 12, 1–10.
Xu, C., Xu, X., Ju, C., Chen, H.Y., Wilsey, B.J., Luo, Y., Fan, W., 2021. Long-term, amplified responses of soil organic carbon to nitrogen addition worldwide. Global Change Biology 27, 1170–1180.
Yang, Y., Dou, Y., Wang, B., Wang, Y., Liang, C., An, S., Soromotin, A., Kuzyakov, Y., 2022. Increasing contribution of microbial residues to soil organic carbon in grassland restoration chronosequence. Soil Biology and Biochemistry 170, 108688.
Yuan, Y., Li, Y., Mou, Z., Kuang, L., Liu, Z., 2020. Phosphorus addition decreases microbial residual contribution to soil organic carbon pool in a tropical coastal forest. Global Change Biology 27, 454–466.
Zhang, T.a., Chen, H.Y., Ruan, H., 2018. Global negative effects of nitrogen deposition on soil microbes. ISME 12, 1817–1825.
Zhang, W., Cui, Y., Lu, X., Bai, E., He, H., Xie, H., Liang, C., Zhang, X., 2016. High nitrogen deposition decreases the contribution of fungal residues to soil carbon pools in a tropical forest ecosystem. Soil Biology and Biochemistry 97, 211–214.
Zhang, X., Amelung, W., 1996. Gas chromatographic determination of muramic acid, glucosamine, mannosamine, and galactosamine in soils. Soil Biology and Biochemistry 28, 1201–1206.
Zhang, Z., Kaye, J.P., Bradley, B.A., Amsili, J.P., Suseela, V., 2022. Cover crop functional types differentially alter the content and composition of soil organic carbon in particulate and mineral-associated fractions. Global Change Biology 28, 5831–5848.